PHYSICAL ELECTRONICS

Original article
DOI: https://doi.org/10.18721/JPM.15310

SIMULATION OF AN ELECTRON BEAM IN A GYROTRON TAKING INTO ACCOUNT THE CATHODE SURFACE ROUGHNESS AND THERMAL EFFECTS IN THE ELECTRON GUN

O. I. Louksha✉, *P. A. Trofimov*, *A. G. Malkin*

Peter the Great St. Petersburg Polytechnic University, St. Petersburg, Russia

✉ louksha@rphf.spbstu.ru

Abstract. In the paper, a 3D trajectory analysis taking into account the surface roughness of the thermionic cathode and thermal effects caused by its heating has been performed in the electron-optical system of a gyrotron with a frequency of 74,2 GHz and an output power of approximately 100 kW. A new approach based on the use of standard settings available in the 3D simulation software when the model parameters of thermionic emission being given, was used for consideration of the micron-sized cathode surface roughness. A comparison between the calculated and experimental data made it possible to clarify the regularities of the influence of the initial velocity spread and the change of geometry of the cathode assembly caused by its heating on the parameters of the electron beam formed in the electron-optical gyrotron system.

Keywords: microwave electronics, gyrotron, helical electron beam, cathode, surface roughness, heating

Funding: The reported study was funded by Russian Science Foundation (Grant No. 22-29-00136). The results were obtained using the computing resources of the Supercomputer Center of the Peter the Great St. Petersburg Polytechnic University (http://www.scc.spbstu.ru).

Citation: Louksha O. I., Trofimov P. A., Malkin A. G., Simulation of an electron beam in a gyrotron taking into account the cathode surface roughness and thermal effects in the electron gun, St. Petersburg State Polytechnical University Journal. Physics and Mathematics. 15 (3) (2022) 132–142. DOI: https://doi.org/10.18721/JPM.15310

This is an open access article under the CC BY-NC 4.0 license (https://creativecommons.org/licenses/by-nc/4.0/)

© Louksha O. I., Trofimov P. A., Malkin A. G., 2022. Published by Peter the Great St. Petersburg Polytechnic University.

Научная статья
УДК 621.385.6
DOI: https://doi.org/10.18721/JPM.15310

МОДЕЛИРОВАНИЕ ЭЛЕКТРОННОГО ПОТОКА В ГИРОТРОНЕ С УЧЕТОМ ШЕРОХОВАТОСТИ ПОВЕРХНОСТИ КАТОДА И ТЕПЛОВЫХ ЭФФЕКТОВ В ЭЛЕКТРОННОЙ ПУШКЕ

О. И. Лукша✉, *П. А. Трофимов*, *А. Г. Малкин*

[1] Санкт-Петербургский политехнический университет Петра Великого,

Санкт-Петербург, Россия

✉ louksha@rphf.spbstu.ru

Аннотация. Выполнен трехмерный траекторный анализ в электронно-оптической системе гиротрона с частотой 74,2 ГГц и выходной мощностью примерно 100 кВт, с учетом шероховатости поверхности термоэмиссионного катода и тепловых эффектов, вызванных его нагревом. Для учета шероховатостей поверхности катода микронного размера использован новый подход, основанный на использовании стандартных инструментов, доступных в программе трехмерного моделирования при задании параметров термоэлектронной эмиссии. Сопоставление расчетных данных с экспериментальными позволили уточнить закономерности влияния разброса начальных скоростей и изменения геометрии катодного узла при его нагреве на параметры электронного потока, формируемого в электронно-оптической системе гиротрона.

Ключевые слова: СВЧ электроника, гиротрон, винтовой электронный поток, катод, шероховатость поверхности, нагрев

Финансирование: Исследование выполнено при финансовой поддержке гранта Российского научного фонда (проект № 00136-29-22). Часть результатов была получена с использованием вычислительных ресурсов суперкомпьютерного центра СПбПУ (http://www.scc.spbstu.ru).

Ссылка для цитирования: Лукша О. И., Трофимов П. А., Малкин А. Г. Моделирование электронного потока в гиротроне с учетом шероховатости поверхности катода и тепловых эффектов в электронной пушке // Научно-технические ведомости СПбГПУ. Физико-математические науки. 2022. Т. 15. № 3. С. 132–142. DOI: https://doi.org/10.18721/JPM.15310

Статья открытого доступа, распространяемая по лицензии CC BY-NC 4.0 (https://creativecommons.org/licenses/by-nc/4.0/)

Introduction

Gyrotrons have become the predominant source of powerful microwave radiation in the millimeter and submillimeter wavelength ranges. In particular, they are used for heating high-temperature plasma and current drive in controlled thermonuclear fusion devices, requring gyrotrons with megawatt levels of output power, operating in continuous and long-pulse modes [1 – 3]. The efficiency of these devices and their maximum achievable parameters depend on the quality of helical electron beam (HEB) entering the resonator. HEB parameters are determined during the design stage through numerical trajectory analysis in the electron-optical system (EOS). The most common type is an adiabatic system including a magnetron injection gun (MIG) with a thermionic cathode and a magnetic compression region [3, 4].

A high-quality HEB is characterized by high mean pitch $\alpha = v_\perp / v_\parallel$ ($v_\perp$, $v_\parallel$ are the transverse and longitudinal velocities of electrons), low velocity ($\delta v_\perp$) and energy ($\delta\varepsilon$) spreads, a specific spatial structure, no parasitic oscillations of the space charge (see, for example, monograph [4]). A major

© Лукша О. И., Трофимов П. А., Малкин А. Г., 2022. Издатель: Санкт-Петербургский политехнический университет Петра Великого.

factors leading to degradation in the quality of HEB is associated with roughness of the cathode surface where the typical sizes of inhomogeneities range from units to tens of microns [4 – 11]. Three-dimensional trajectory analysis can be complicated in a system whose cathode surface has inhomogeneities of similar size. As gyrotron EOSs are typically hundreds of millimeters long, a mesh accounting for such a cathode has a large number of cells, which is unacceptable for modern computational systems. Different algorithms have been developed to implicitly take into account the roughness of the emitting surface in the EOS model with a smooth cathode by setting the initial velocity of each particle emitted from the cathode [10, 11]. These algorithms rely on data from preliminary computations, performed separately for each specific gyrotron.

In practice, disagreement is often observed between the theoretical and experimental values of HEB parameters; to avoid this, trajectory analysis should take into account the possible variations in MIG geometry due to heating of the thermionic cathode. Accounting for thermal effects in an electron gun is also a problem specific to each particular device with its characteristic dimensions of EOS elements.

The method we adopt in this paper to account for the cathod roughness during computations of electron trajectories in gyrotron EOS is simpler compared to the approaches in [10, 11]. We used tools from the CST Studio Suite [12] available for setting the parameters of thermionic emission. The suite was used for all computations described in the paper. The computations yielded the HEB characteristics in the EOS of the gyrotron at Peter the Great St. Petersburg Polytechnic University with an operating frequency of 74.2 GHz and an output power of ~100 kW [13 – 16], helping establish the influence of the emitter's surface roughness and heating on these characteristics.

Cathode model with rough surface and effect of roughness on HEB parameters

The electrons emitted from the MIG cathode acquire an initial transverse velocity under the action of crossed electric and magnetic fields. Following the adiabatic theory of MIG (see, for example, [4, 5]), we assume that the transverse electron velocity near the cathode is expressed as

$$v_{\perp c} = \overline{v_{\perp c}} \pm v_\theta, \tag{1}$$

where $\underline{v}_{\perp c} = E_{\perp c}/B_c$ is the mean transverse velocity in the cathode; $E_{\perp c}$ is the component of the electric field near the cathode, perpendicular to the magnetic field; B_c is the induction of the magnetic field near the cathode; v_θ is the initial velocity magnitude in the direction perpendicular to the magnetic field (coincides with the azimuthal direction for the axially symmetric gyrotron EOS).

If the cathode has a rough surface, the electrons acquire initial velocities under the action of microfields near local inhomogeneities on this surface. As a result, a spread of the initial transverse velocities of electrons is observed in the cathode:

$$\delta v_{\perp c} = \frac{\Delta v_\theta}{\overline{v_{\perp c}}}, \tag{2}$$

where Δv_θ is the absolute spread of the initial velocities.

In addition to roughness, another factor leading to an increase in $\delta v_{\perp c}$ is the spread in the initial thermal velocities of electrons emitted from the surface of the cathode. Importantly, the magnitude of the relative spread in transverse velocities accounting for all factors of this spread remains unchanged as HEB moves in an adiabatically increasing magnetic field, which is used for pumping the transverse electron velocity in the gyrotron EOS.

The velocity distributions of electrons in a model of a planar diode without a magnetic field are compared in [17] with two types of cathodes: the first one has a rough surface with regularly spaced hemispheres of radius r_0, and the second one has a smooth surface.

The electron distribution $f(v_x)$ (x is the coordinate along its surface) for the first type of cathode practically does not change with increasing distance z from the cathode, if it exceeds a value equal to approximately $2r_0$. It was established that the initial velocity spectra of cathodes with the rough surface are in satisfactory agreement with those of the cathode with the smooth surface, if a Maxwell distribution of the emitted particle velocities is given for the former, namely

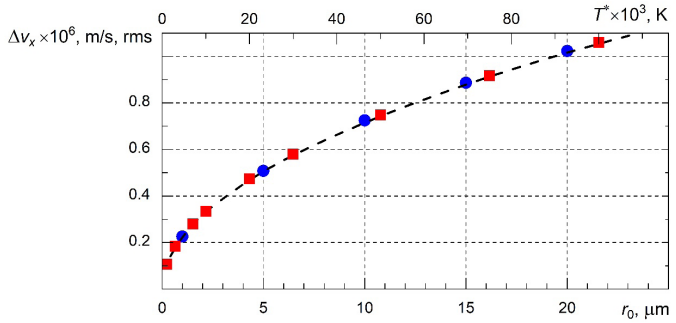

Fig. 1. Dependences of the spread in velocities of electrons emitted from the cathode on the radius r_0 in the model with the rough cathode (−●−) and on the effective temperature T^* in the model with a smooth cathode (−■−) with a macroscopic field strength of 30 kV/cm in the cathode-anode gap

$$f(v)dv = 4\pi v^2 \left(\frac{m}{2\pi kT}\right)^{3/2} \exp\left(-\frac{mv^2}{2kT}\right) dv, \qquad (3)$$

with the temperature T^* appreciably higher than the actual cathode temperature T_c, if the azimuth angles $\Delta\theta$ are set between the normal to the cathode surface and the direction of the initial velocity vector equal to ±90°. Fig. 1 shows the dependences for the spread in initial velocities Δv_x on the effective temperature T^* for the model with a smooth cathode and on the radius r_0 for the model with a rough cathode. The spread in electron velocities here and below is defined as the root-mean-square (rms) deviation from the mean velocity. The values of Δv_x for the rough cathode model were obtained after averaging the initial velocity spectra calculated for different distances between the hemispheres at a given radius r_0. If we assume that r_0 = 10 μm corresponds to $T^* = 46 \cdot 10^3$ K, then the dependences $\Delta v_x(r_0)$ and $\Delta v_x(T^*)$ almost coincide (see Fig. 1).

Notably,the cathode in an axially symmetric EOS is cone-shaped and there is a magnetic field near it [4]. As noted above, the velocity v_x changes at a short distance from the cathode, not exceeding several radii r_0. At this distance, the electron motion has little difference with the motion in a planar diode. Moreover, the influence of the magnetic field on this motion is insignificant [4]. Therefore, the calculated velocity spread Δv_x can be regarded as the spread in the initial transverse velocity $\Delta v_{\perp c}$. Since the temperature $T^* >> T_c$ for typical values of r_0, the spread in the initial velocities Δv_x, calculated from the temperature T^*, can be attributed to the total effect induced by the surface roughness of the cathode and the spread of thermal velocities.

Table 1

Main geometric parameters and characteristics of computational operating mode in SPbPU gyrotron

Parameter	Value
Accelerating voltage U_0, kV	30
Beam current I_b, A	10
Magnetic field induction in the cavity B_0, T	2.75
Magnetic field induction near cathode B_c, T	0.152
Operating mode	$TE_{12.3}$
Mean radius of emissive strip in the cathode R_c, mm	35
Distance between cathode and anode D_{ca}, mm	10.4
Slant angle of conical emissive strip to device axis, ψ_c, deg	35
Slant angle of magnetic field line to cathode surface ϕ_c, deg	19.2

The approach to accounting for cathode roughness proposed in [17], based on an EOS model with a smooth cathode and setting the distribution of initial velocities (3) with the given values of the parameters T^* and $\Delta\theta$, was also used in our study to perform trajectory analysis for the gyrotron at SPbPu during operation [13 – 16]. The main parameters of this gyrotron are presented in Table 1. The image of gun region in this gyrotron is shown below in Figs. 3 and 4. If we select the velocity spread $\Delta v_{\perp c} = 7.25 \bullet 10^5$ m/s, which corresponds to $r_0 = 10$ μm (see Fig. 1), then, according to (1) and (2), the spread in the initial transverse velocities in the cathode $\delta v_{\perp c}$ for the values of U_0, B_c, D_{ca}, ψ_c, φ_c given in Table 1 is equal to 3.63% due to the cathode's roughness.

Two configuration of the magnetron injection gun were used in the calculations [18]. The slant angle of the conical part of the cathode, equal to 35°, was the same along the entire generatrix in the standard gun configuration. The gyrotron operates with the mean pitch $_|$ equal to approximately 1.3 for the gun with the parameters given in Table 1. The values of the pitch α and the velocity spread $\delta v_\perp$ discussed in this paper were determined in the central plane of the resonator for the peak of the magnetic field distribution along the longitudinal coordinate. A control electrode was installed Ii the modified version of the gun, with the inclination angle of the conical part increased to 50°. Earlier studies [19] indicate that controlling the voltage between the cathode and the control electrode U_{cont} can help optimize the distribution of the electric field in the near-cathode region of the MIG, consequently reducing the velocity spread in the beam. This allows increasing the working pitch and the efficiency of the gyrotron [20].

Trajectory analysis was carried out with the model of the SPbPU gyrotron, described in detail in [18]. The number of emission centers was increased to about $3 \cdot 10^4$, producing smoother velocity distributions of electrons at higher temperatures of the cathode. Tracking Solver was used to calculate the trajectories. The dependences of the mean pitch α and the velocity spread $\delta v_\perp$ on the effective temperature T^* for two configurations of the MIG are shown in Fig. 2. An increase in $\delta v_\perp$ is observed with the increase in temperature T^*. Provided that $T^* \approx 0$, the velocity spread is due to the difference in the values of external electrical and magnetic fields, as well as the intrinsic field of the HEB space charge for electrons starting from different points of the emitter. This spread in positions is smaller for the modified MIG for the optimal value $U_{cont} = -9$ kV compared to the standard MIG. It is then self-evident why introducing an additional spread of initial velocities produces a more noticeable increase in the total velocity spread for a gyrotron with a modified MIG.

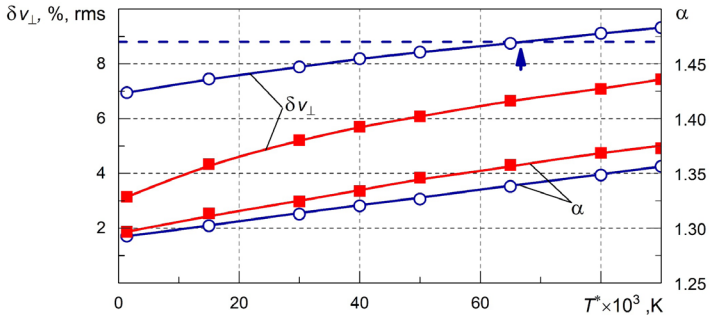

Fig. 2. Dependences of transverse velocity spread $\delta v_\perp$ and the mean pitch α on the effective temperature T^* for standard (–○–) and modified (–■–) magnetron injection gun; $U_{cont} = -9$ kV

Experimental data obtained earlier at the SPbPU gyrotron with a standard MIG [21] suggest that the velocity spread $\delta v_\perp$ is approximately 8.8% for a cathode with uniform emission. This spread value was recorded in particular in experiments with a cathode made of lanthanum hexaboride (LaB_6), whose active substance has typical particle sizes of about 10 μm. The active substance can escape from the surface of the emitter as the cathode operates. This partially exposes a sponge whose grain size may be noticeably larger than the particle size in the lanthanum hexaboride powder. An additional consideration is that the area of the emitting surface is also rather large, about 10 cm^2. This surface may be inhomogeneous, which is due to uneven heating and non-uniform beams of the particles bombarding the cathode surface. In view of these factors,

we can assume that the size of the roughnesses appearing on the cathode during measurements (determining the magnitude of the spread in the initial velocities $\delta v_{\perp c}$) is different from that of the particles in the active substance of the emitter. As evident from Fig. 2, the spread $\delta v_{\perp} = 8.8\%$ is achieved for a standard MIG at $T^* \approx 67 \cdot 10^3$ K. We can therefore conclude from the dependences in Fig. 1 that the LaB6 cathode for which a velocity spread of 8.8% was recorded in the experiments was characterized by a mean roughness with a radius $r_0 \approx 14$ μm.

Simulation of thermal effects associated with cathode heating

The model of the SPbPU gyrotron used in the calculations of the temperature distribution is shown in Fig. 3. Cathode *1* of the device can be disassembled, allowing to easily replace component *2* with the emitting strip. The cathode is heated with tungsten heating coil *3*. Filament current I_h of the heater flows along central core *4* of the cathode. Thermal shields and special gaps between the components provide thermal insulation of the heating coil and the emitting strip from the remaining elements of the cathode assembly. More than ten emitters of two types were used in the SPbPU gyrotron at different stages of the study: porous tungsten-barium (operating temperature $T_c \approx 1100$ °C) and lanthanum hexaboride ($T_c \approx 1600$ °C) [22].

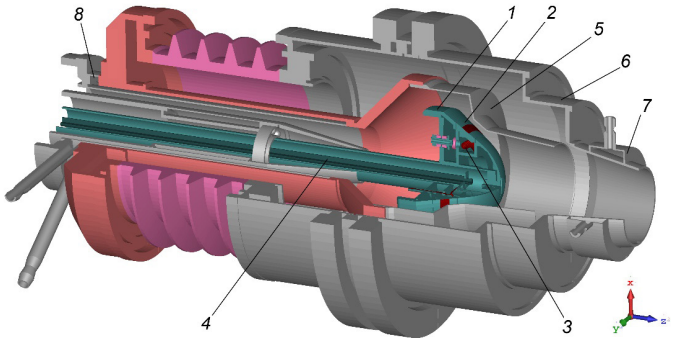

Fig. 3. 3D image of SPbPU gyrotron gun:
cathode assembly *1*; component with emitting strip *2*;
coil *3*; central core *4*; anode *5*; vessel *6*; water cavities *7*, *8*

The problem on determining the deformation of MIG elements due to heating of the thermionic cathode was solved in three stages. During the first stage, we calculated the current density in the heater circuit using the Stationary Current Solver accounting for the conductive properties of the materials and the geometry of the elements in the cathode assembly. The data obtained were used to calculate the amount of heat released during ohmic heating of conductive components with the current I_h flowing through them.

During the second stage, we calculated the steady-state temperature distribution with the Thermal Static Solver. In addition to ohmic heating considered in the first stage, we acconted for the radiation of heated bodies which are secondary sources of heat in the vacuum system. We determined the losses of heated bodies assumed to be additional heat sources for bodies absorbing thermal radiation. Fig. 4 shows the temperature distribution in the cathode assembly of the gyrotron at a current $I_h = 30$ A, corresponding to heating of the cathode made of lanthanum hexaboride. Evidently, the most heated elements are the ones in the cathode assembly. The thermal deformation associated with their heating can modify the geometry of the MIG and, as a result, lead to changes in the parameters of the electron beam generated.

At the third stage, the thermal strains were calculated with the Linear Structural Mechanics Solver allowing to find the parameters characterizing the linear and volumetric expansion of solids. The cathode stem used for attaching the cathode is connected to the gyrotron vessel through the insulator in the end area of the gyrotron (see Fig. 3). Therefore, the cathode is shifted towards the resonator due to linear expansion of the elements of the cathode assembly in the longitudinal direction. Volumetric expansion is accompanied by an increase in the mean radius of the emitting strip. The values of the corresponding parameters Δz and Δr, which were calculated at filament currents I_h, required for heating LaB_6 and W-Ba cathodes, are given in Table 2.

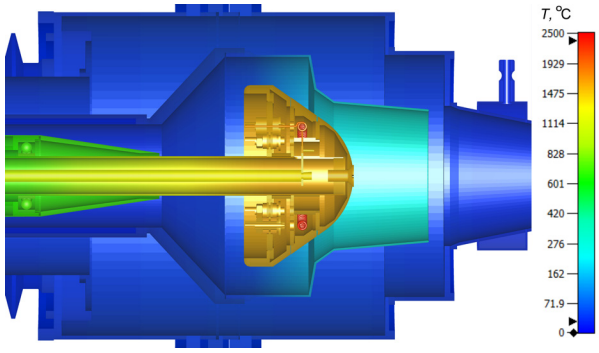

Fig. 4. Simulated temperature distribution across gyrotron elements with lanthanum hexaboride cathode

Table 2

Deformation of MIG elements for two types of thermal cathode

Operating characteristics of MIG			Variation in MIG geometry	
Material of cathode	I_h	T_c	Δz	Δr
	A	°C	mm	
LaB_6	30	1616	1.41	0.29
W-Ba	25	1100	0.98	0.21

Notations: I_h is the filament current, T_c is the cathode temperature, Δz is the longitudinal displacement of the cathode, Δr is the radial expansion of the emissive strip, MIG is the magnetron injection gun.

The electron trajectories were computed depending on the values of the parameters Δz and Δr for the modified MIG, since its geometry was optimized to obtain a minimum velocity spread. Initially, the cathode temperature was set equal to T_c, that is, only the spread in the initial thermal velocities of electrons exclusive of cathode roughness was taken into account. The dependences of the mean pitch α and the velocity spread $\delta v_\perp$ on the parameters Δz and Δr are shown in Fig. 5. Only the change in the sizes of the cathode assembly component with the emitting strip was taken into account for varying Δr, (see Fig. 3).

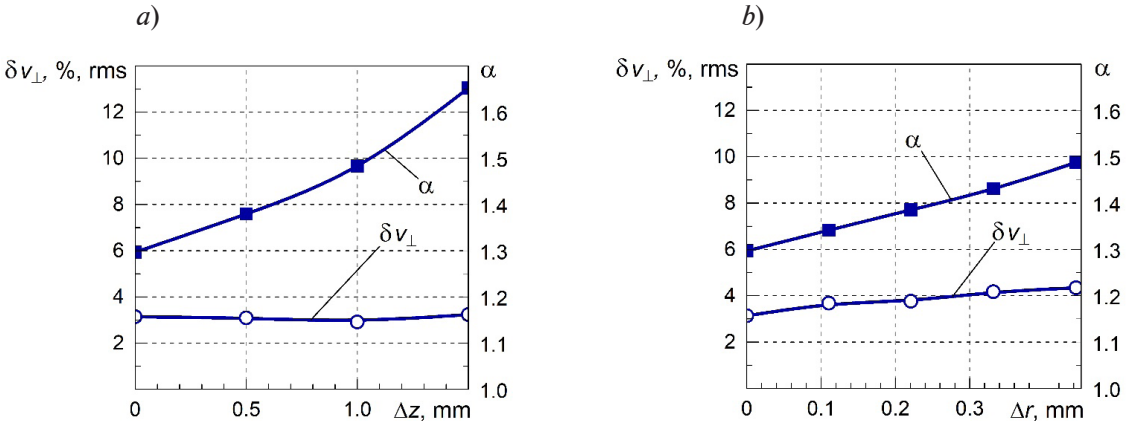

Fig. 5. Dependences of the spread in transverse velocities $\delta v_\perp$ and the mean pitch α on the longitudinal displacement Δz (*a*) of the cathode and on the radial expansion Δr (*b*) of the emitting strip for the modified MIG; $U_{cont} = -9$ kV

Elongation of the cathode stem leads to a reduction in the distance between the cathode and the anode, consequently increasing the amplitude of the electrical field in this region. As a result, the initial transverse velocity in the cathode and the mean pitch increase. The distribution of the electric field (the form of equipotentials) remains virtually invariable with varying Δz. Since the magnitude of the velocity spread depends mainly on this distribution , it also varies insignificantly with varying Δz. The increase in α with growing Δr can also be explained by a reduction in the distance between the cathode and the anode. The radial expansion of the component with the emitting strip is accompanied by some change in the distribution of the electric field. Since this distribution was optimized in the initial state ($\Delta r = 0$) to obtain a minimum velocity spread, any variation in this distribution is accompanied by an increase in the value of $\delta v_{\perp}$ (Fig. 5, *b*).

As the final stage of the study, we carried out trajectory analysis for the SPbPU gyrotron with a modified MIG accounting for both cathode roughness and the thermal effects due to its heating. We considered a temperature regime corresponding to the cathode made of lanthanum hexaboride. Given that $\Delta z = 1.41$ mm, $\Delta r = 0.29$ mm, $T^* = 67 \cdot 10^3$ K and $\Delta\theta = \pm 90°$, we obtained the following values of the mean pitch factor and velocity spread: $\alpha = 2.25$ and $\delta v_{\perp} = 5.89\%$. A marked increase in the pitch compared to the initial value $\alpha \approx 1.3$ (see Fig. 2) occurred due to simultaneous elongation of the cathode stem and expansion of the emitting strip. At large values of α and $\delta v_{\perp}$, a part of electrons with largeand transverse velocities is reflected from the magnetic plug in the region before entering the resonator (see, for example, articles [18, 21]). The reflected particles can accumulate in the trap between the cathode and the magnetic mirror, which is accompanied by excitation of parasitic low-frequency oscillations (LFO) negatively affecting the quality of the HEB generated. In the above-described configuration, 364 particles out of 30,120 starting from the cathode were reflected from the magnetic mirror. This corresponds to the reflection coefficient $K_{refl} = 1.2 \cdot 10^{-2}$. Parasitic LFO with a considerable amplitude can be excited with such a reflection coefficient [21].

The values of α and K_{refl} can be decreased by increasing the magnetic field induction B_c near the cathode and, accordingly, reducing the magnetic compression coefficient B_0/B_c. The values of the main parameters U_0, B_0 and I_b primarily determining the generated power and radiation frequency remain unchanged. The magnetic field near the cathode of the SPbPU gyrotron can be increased by increasing the number of turns of the cathode coil [22]. The results described above for the modified MIG were obtained for $B_0/B_c = 19.20$, which corresponds to 22 turns of the cathode coil. Adopting the configuration with 24 turns is accompanied by a decrease in B_0/B_c to 18.02. The values of the pitch and the velocity spread calculated with this B_0/B_c amounted to $\alpha = 1.44$ and $\delta v_{\perp} = 6.59\%$. These values indicate that HEB has high quality, with no electron reflection from the magnetic mirror, and improved performance of the gyrotron with a large value of electronic efficiency [20].

Conclusion

The new technique proposed in this paper can be used to account for the spread of the initial electron velocities due to roughness of the cathode surface during 3D simulations of electron trajectories in the electron-optical system of the gyrotron. We have determined the effect of cathode roughness on the velocity spread and the mean pitch of electrons in the EOS of a medium-power 4 mm gyrotron. Comparing the data obtained in the experiment with the results of trajectory analysis, we have determined the average size of inhomogeneities on the surface of the cathode used in this gyrotron.

We have acquired data characterizing the heating of various EOS elements at operating temperatures of thermionic cathodes used in the gyrotron. The effects of cathode stem elongation and radial expansion of the emitting strip on HEB parameters have been determined. It was confirmed that the gyrotron can generate high-quality HEBs in an operational mode accounting the relationship of its parameters with cathode roughness and thermal effects in the electron gun.

REFERENCES

1. **Litvak A. G., Denisov G. G., Myasnikov V. E., et al.,** Development in Russia of megawatt power gyrotrons for fusion, J. Infrared Millim. Terahertz Waves. 32 (3) (2011) 337–342.

2. **Thumm M.,** State-of-the-art of high-power gyro-devices and free electron masers, J. Infrared Millim. Terahertz Waves. 41 (1) (2020) 1–140.

3. **Nusinovich G. S.,** Introduction to physics of gyrotrons, Johns Hopkins University Press, Baltimore, USA, 2004.

4. **Tsimring Sh. E.,** Electron beams and microwave vacuum electronics, John Wiley & Sons, Hoboken, 2007.

5. **Tsimring Sh. E.,** On the spread of velocities in helical electron beams, Radiophys. Quant. El. 15 (8) (1972) 952–961.

6. **Avdoshin E. G., Nikolaev L. V., Platonov I. N., Tsimring Sh. E.,** Experimental investigation of the velocity spread in helical electron beams, Radiophys. Quant. El. 16 (4) (1973) 461–466.

7. **Lau Y. Y.,** Effects of cathode surface roughness on the quality of electron beams, J. Appl. Phys. 61 (1) (1987) 36–44.

8. **Lygin V. K.,** Numerical simulation of intense helical electron beams with the calculation of the velocity distribution functions, Int. J. Infrared Millim. Waves. 16 (2) (1995) 363–376.

9. **Zapevalov V. E., Kornishin S. Yu., Kotov A. V., et al.**, System for the formation of an electron beam in a 258 GHz gyrotron designed for experiments on dynamic polarization of nuclei, Radiophys. Quant. El. 53 (4) (2010) 229–236.

10. **Leshcheva K. A., Manuilov V. N.,** Numerical simulation of 3-D systems of formation of helical electron beams of gyro-devices with azimutally inhomogeneous distribution of emission current, Advances in Applied Physics. 7 (3) (2019) 298–308 (in Russian).

11. **Zhang J., Illy S., Pagonakis I., Avramidis K., et al.,** Influence of emitter surface roughness on high power fusion gyrotron operation, Nucl. Fusion. 56 (2) (2016) 026002.

12. CST Studio Suite, URL: https://www.3ds.com/products-services/simulia/ products/cst-studio-suite/. Accessed July 06, 2022.

13. **Kas'yanenko D. V., Louksha O. I., Sominsky G. G., et al.,** Low-frequency parasitic space-charge oscillations in the helical electron beam of a gyrotron, Radiophys. Quant. El. 47 (5–6) (2004) 414–420.

14. **Louksha O. I., Piosczyk B., Sominski G. G., et al.,** Suppression of parasitic space-charge oscillations in a gyrotron, Radiophys. Quant. El. 49 (10) (2006) 793–798.

15. **Louksha O. I.,** Simulation of low-frequency collective processes in gyrotron electron beams, Radiophys. Quant. El. 52 (5–6) (2009) 386–397.

16. **Louksha O. I., Sominski G. G., Arkhipov A. V., et al.,** Gyrotron research at SPbPU: Diagnostics and quality improvement of electron beam, IEEE Trans. Plasma Sci. 44 (8) (2016) 1310–1319.

17. **Louksha O. I., Trofimov P. A., Malkin A. G.,** Vliyaniye sherokhovatosti poverkhnosti katoda na kharakteristiki elektronnogo potoka v elektronno-opticheskoy sisteme girotrona [Effect of cathode surface roughness on the characteristics of the electron beam in the electron optical system of a gyrotron], In book: XI Vserossiyskaya nauchno-tekhnicheskaya konferentsiya "Elektronika i mikroelektronika SVCH". Sbornik dokladov [Transactions of XI All-Russian Scientific and Technical Conference "Electronics and Microelectronics of Microwaves", May 31 – June 3, 2022, St. Petersburg, Russia. The collection of reports, ETU "LETI", St. Petersburg (2022) 562–566 (in Russian).

18. **Louksha O. I., Trofimov P. A.,** Simulation of non-uniform electron beams in the gyrotron electron-optical system, Tech. Phys. 63 (4) (2018) 598–604.

19. **Louksha O. I., Samsonov D. B., Sominskii G. G., Tsapov A. A.,** Improvement of the helical electron beam quality and the gyrotron efficiency by controlling the electric field distribution near a magnetron injection gun, Tech. Phys. 57 (6) (2012) 835–839.

20. **Louksha O. I., Trofimov P. A.,** Highly efficient gyrotron with multi-stage recuperation of residual electron energy, Tech. Phys. 64 (12) (2019) 1889–1897.

21. **Louksha O. I., Samsonov D. B., Sominskii G. G., Semin S. V.,** Dynamic processes in helical electron beams in gyrotrons, Tech. Phys. 58 (5) (2013) 751–759.

22. **Louksha O. I., V**intovye elektronnye potoki girotronov: dinamika prostranstvennogo zaryda i metody povysheniya kachestva [Gyrotron helical electron beams: Space charge dynamics and methods for quality improvement], Thesis for a Doctor's degree (phys.-math. sci.), St. Petersburg, SPbPU, 2011.

СПИСОК ЛИТЕРАТУРЫ

1. **Litvak A. G., Denisov G. G., Myasnikov V. E., Tai E. M., Azizov E. A., Ilin V. I.** Development in Russia of megawatt power gyrotrons for fusion // Journal of Infrared, Millimeter, and Terahertz Waves. 2011. Vol. 32. No. 3. Pp. 337–342.

2. **Thumm M.** State-of-the-art of high-power gyro-devices and free electron masers // Journal of Infrared, Millimeter, and Terahertz Waves. 2020. Vol. 41. No. 1. Pp. 1–140.

3. **Nusinovich G. S.** Introduction to physics of gyrotrons. Baltimore, USA: Johns Hopkins University Press, 2004. 335 p.

4. **Цимринг Ш. Е.** Введение в высокочастотную вакуумную электронику и физику электронных пучков. Пер. с англ. Нижний Новгород: Ин-т прикладной физики РАН, 2012. 575 с.

5. **Цимринг Ш. Е.** О разбросе скоростей в винтовых электронных пучках // Известия вузов. Радиофизика. 1972. Т. 15. № 8. С. 1247–1259.

6. **Авдошин Е. Г., Николаев Л. В., Платонов И. М., Цимринг Ш. Е.** Экспериментальное исследование скоростного разброса в винтовых электронных пучках // Известия вузов. Радиофизика. 1973. Т. 16. № 4. С. 605–612.

7. **Lau Y. Y.** Effects of cathode surface roughness on the quality of electron beams // Journal of Applied Physics. 1987. Vol. 61. No. 1. Pp. 36–44.

8. **Lygin V. K.** Numerical simulation of intense helical electron beams with the calculation of the velocity distribution functions // International Journal of Infrared and Millimeter Waves. 1995. Vol. 16. No. 2. Pp. 363–376.

9. **Запевалов В. Е., Корнишин С. Ю., Котов А. В., Куфтин А. Н., Малыгин О. В., Мануилов В. Н., Седов А. С., Цалолихин В. И.** Система формирования электронного пучка для гиротрона с частотой 258 ГГц, предназначенного для экспериментов по динамической поляризации ядер // Известия вузов. Радиофизика. 2010. Т. 53. № 4. С. Р. 251–259.

10. **Лещева К. А., Мануилов В. Н.** Численное 3D-моделирование систем формирования винтовых электронных пучков гироприборов с азимутально неоднородным распределением тока эмиссии // Успехи прикладной физики. 2019. Т. 7. № 3. С. 298–308.

11. **Zhang J., Illy S., Pagonakis I., Avramidis K., Thumm M., Jelonnek J.** Influence of emitter surface roughness on high power fusion gyrotron operation // Nuclear Fusion. 2016. Vol. 56. No. 2. P. 026002.

12. CST Studio Suite. Режим доступа: https://www.3ds.com/products-services/simulia/products/cst-studio-suite/ (Дата обращения: 17.06.2022).

13. **Касьяненко Д. В., Лукша О. И., Пиосчик Б., Соминский Г. Г., Тумм М.** Низкочастотные паразитные колебания пространственного заряда в винтовом электронном пучке гиротрона // Известия вузов. Радиофизика. 2004. Т. 47. № 5–6. С. 463–470.

14. **Лукша О. И., Пиосчик Б., Соминский Г. Г., Тумм М., Самсонов Д. Б.** Подавление паразитных колебаний пространственного заряда в гиротроне // Известия вузов. Радиофизика. 2006. Т. 49. № 10. С. 880–886.

15. **Лукша О. И.** Моделирование низкочастотных коллективных процессов в электронных потоках гиротронов // Известия вузов. Радиофизика. 2009. Т. 52. № 5–6. С. 425–437.

16. **Louksha O. I., Sominski G. G., Arkhipov A. V., Dvoretskaya N. V., Kolmakova N. G., Samsonov D. B., Trofimov P. A.** Gyrotron research at SPbPU: Diagnostics and quality improvement of electron beam // IEEE Transactions on Plasma Science. 2016. Vol. 44. No. 8. Pp. 1310–1319.

17. **Лукша О. И., Трофимов П. А., Малкин А. Г.** Влияние шероховатости поверхности катода на характеристики электронного потока в электронно-оптической системе гиротрона // XI Всероссийская научно-техническая конференция «Электроника и микроэлектроника СВЧ». 31 мая – 3 июня 2022 г., г. Санкт-Петербург, Россия. Сборник докладов. СПб.: СПбГЭТУ «ЛЭТИ», 2022. С. 562–566.

18. **Лукша О. И., Трофимов П. А.** Моделирование неоднородных электронных потоков в электронно-оптической системе гиротрона // ЖТФ. 2018. Т. 88. № 4. С. 614–620.

19. **Лукша О. И., Самсонов Д. Б., Соминский Г. Г., Цапов А. А.** Повышение качества винтового электронного потока и КПД гиротрона при регулировании распределения электрического поля в области магнетронно-инжекторной пушки // ЖТФ. 2012. Т. 82. № 6. С. 101–105.

20. **Лукша О. И., Трофимов П. А.** Высокоэффективный гиротрон с многоступенчатой рекуперацией остаточной энергии электронов // ЖТФ. 2019. Т. 89. № 12. С. 1988–1996.

21. **Лукша О. И., Самсонов Д. Б., Соминский Г. Г., Семин С. В.** Динамические процессы в винтовых электронных потоках гиротронов // ЖТФ. 2013. Т. 83. № 5. С. 132–140.

22. **Лукша О. И.** Винтовые электронные потоки гиротронов: динамика пространственного заряда и методы повышения качества. Дисс. ... докт. физ.-мат. наук. 01.04.04. Защ. 01 декабря 2011 г.: утв. 01.12.2011. СПб.: СПбГПУ, 2011. 285 с.

THE AUTHORS

LOUKSHA Oleg I.
Peter the Great St. Petersburg Polytechnic University
29 Politechnicheskaya St., St. Petersburg, 195251, Russia
louksha@rphf.spbstu.ru
ORCID: 0000-0002-6402-8112

TROFIMOV Pavel A.
Peter the Great St. Petersburg Polytechnic University
29 Politechnicheskaya St., St. Petersburg, 195251, Russia
trofpa@yandex.ru
ORCID: 0000-0002-3585-1169

MALKIN Alexander G.
Peter the Great St. Petersburg Polytechnic University
29 Politechnicheskaya St., St. Petersburg, 195251, Russia
alexmalkin47@gmail.com
ORCID: 0000-0003-4047-3956

СВЕДЕНИЯ ОБ АВТОРАХ

ЛУКША Олег Игоревич – *доктор физико-математических наук, профессор Высшей инженерно-физической школы Санкт-Петербургского политехнического университета Петра Великого.*
195251, Россия, г. Санкт-Петербург, Политехническая ул., 29
louksha@rphf.spbstu.ru
ORCID: 0000-0002-6402-8112

ТРОФИМОВ Павел Анатольевич – *кандидат физико-математических наук, инженер Высшей инженерно-физической школы Санкт-Петербургского политехнического университета Петра Великого.*
195251, Россия, г. Санкт-Петербург, Политехническая ул., 29
trofpa@yandex.ru
ORCID: 0000-0002-3585-1169

МАЛКИН Александр Геннадьевич – *студент Высшей инженерно-физической школы Санкт-Петербургского политехнического университета Петра Великого.*
195251, Россия, г. Санкт-Петербург, Политехническая ул., 29
alexmalkin47@gmail.com
ORCID: 0000-0003-4047-3956

Received 31.05.2022. Approved after reviewing 06.07.2022. Accepted 06.07.2022.
Статья поступила в редакцию 31.05.2022. Одобрена после рецензирования 06.07.2022. Принята 06.07.2022.

© Peter the Great St. Petersburg Polytechnic University, 2022